Supporting Information

Facilitative Functionalization of Cyanine Dye by On-Off-On Fluorescent Switch for Imaging of H_2O_2 Oxidative Stress and Thiols Reducing Repair in Cells and Tissue

Fabiao Yu,[a] Peng Li,[b] Ping Song,[b] Bingshuai Wang,[b] Jianzhang Zhao[a] and Keli Han[b]*

[a]School of Chemical Engineering, Dalian University of Technology, Dalian, 116024, P. R. China; [b]State Key Laboratory of Moleclar Reaction Dynamics, Dalian Institute of Chemical Physics, Chinese Academy of Sciences

E-mail: klhan@dicp.ac.cn

Contents:

1. General Experimental Section

[**Completed ref. 4**]: (a) E.W. Miller, O. Tulyathan, E. Y. Isacoff, C. J. Chang, *Nat. Chem. Biol.* **2007**, 3, 263. (b) B. C. Dickinson, J. Peltier, D. Stone, D. V. Schaffer, C. J. Chang, *Nat. Chem. Biol.* **2011**, 7, 106. (c) D B. C. ickinson, C. J. Chang, *Nat. Chem. Biol.* **2011**, 7, 504. (d) F. Aslund, M. Zheng, J. Beckwith, G. Storz, *Proc. Natl Acad. Sci.* USA, **1999**, 96, 6161.

[**Completed ref. 15**]: (a) A. R. Lippert, G. C. Van de Bittner, C. J. Chang, *Acc Chem Res.* **2011**, 44, 793. (b) P. Niethammer, C. Grabher, A. T. Look, T. J. Mitchison, *Nature* **2009**, 459, 996. (c) H.

Maeda, Y. Fukuyasu, S. Yoshida, M. Fukuda, K. Saeki, H. Matsuno, Y. Yamauchi, K. Yoshida, K. Hirata, K. Miyamoto, *Angew. Chem. Int. Ed.* **2004**, 43, 2389. (d) N. Soh, O. Sakawaki, K. Makihara, Y. Odo, T. Fukaminato, T. Kawai, M. Irie, T. Imato, *Bioorg. Med. Chem.* **2005**, 13, 1131. (e) N. Karton-Lifshin, E. Segal, L. Omer, M. Portnoy, R. Satchi-Fainaro, D. Shabat, *J. Am. Chem. Soc.* **2011**, 133, 10960. (f) M. Abo, Y. Urano, K. Hanaoka, T. Terai, T. Komatsu, T. Nagano, *J. Am. Chem. Soc.* **2011**, 133, 10629. (g) F. Yu, P.Li, P. Song, B. Wang, J. Zhao, K. Han, *Chem. Commun*., **2012**, 48, 2852.

[**Completed ref. 18**]: 18 (a) X. Shen, B. Xia, M. Z. Wrona, G. Dryhurst, *Chem. Res. Toxicol.* **1996**, 9, 1117. (b) F. Zhang, G. Dryhurst, J. Med. Chem. **1994**, 37, 1084. (c) J. P. E. Spencer, P. Jenner, S. E. Daniel, A. J. Lees, D. C. Marsden, B. J. Halliwell, *Neurochem.* **1998**, 71, 2112. (d) J. Yu, W. Wei, E. Danner, R. K. Ashley, J. N. Israelachvili, J. H. Waite, *Nat. Chem. Biol.* **2011**, 7, 588.

Materials: The solution of the probe DA-Cy (acetonitrile, 1.0 mM) could be maintained in refrigerator at 4°C. 2-[4-Chloro-7-(1-ethyl-3,3-dimethyl(indolin-2-ylidene)]-3,5-(propane-1,3-diyl)-1,3,5-heptatrien-1-yl)-1-ethyl-3,3-dimethyl-3H-indolium (Cy.7.Cl) was synthesized in our laboratory.[1] Methyl linoleate (MeLH) and 2,2'-azobis-(2,4-dimethyl)valeronitrile (AMVN) were used to produce MeLOOH.[2] $^1O_2$ was generated by the reaction of H_2O_2 with NaClO,[3] and $O_2^{\cdot-}$ was created by the enzymatic reaction of xanthine/xanthineoxidase (XA/XO; 6.0 μM/3 mU) at 25 ^oC for 5 min.[4] *Tert*-butylhydroperoxide (*t*-BuOOH) and cumene hydroperoxide (CuOOH) could also use to induce ROS in biological systems.[5] ·OH was generated by Fenton reaction between Fe^{II}(EDTA) and H_2O_2 quantitively, and Fe^{II}(EDTA) concentrations represented ·OH concentrations.[6] The cell-permeant SYTO-16 green fluorescent nucleic acid stain (SYTO-16 dye) exhibited bright, green fluorescence upon binding to nucleic acids. The blue fluorescent Hoechst dyes are cell permeable nucleic acid stains. The fluorescence of these dyes is very sensitive to DNA conformation and chromatin state in cells. The regents were purchased from Invitrogen Corporation, and used according to the manufacturer's instructions. All other chemicals were from commercial sources and of analytical reagent grade, unless indicated otherwise. Human normal liver cell line (HL-7702 cells), human hepatoma cell line (HepG2 cells), and the mouse macrophage cell line (RAW264.7 cells) were purchased from the Committee on type Culture Collection of Chinese Academy of Sciences. The hippocampi of 2-days-old rats were purchased from Binzhou Medical University. All experiments were performed in accordance with the guidelines established by the Committee of Animal Research Policy of Binzhou Medical University. Ultrapure water was used throughout. All chemical test solution should be bubbled with argon to deoxygenation before operation.

[1] N. Narayanan, G. Patonay, *J. Org. Chem.* **1995**, *60*, 2391 – 2395.

[2] a) J. A. Terao, A. Nagao, D.-K. Park, B. P. Lim, *Meth. Enzymol.* **1992**, *213*, 454-460; b) B. Chance, H. Sies, A. Boveris, *Proc. Natl. Acad. Sci. U.S.A.* **1988**, *85*, 3175-3179.

[3] Free Radicals in Biology and Medicine. New York, Oxford University Press, **1989**, 58-70.

[4] a) V. Massey, D. J. Edmondson, *Biol. Chem.* **1970**, *245*, 6595-6598; b) D. Edmondson, V. Massey, G. Palmer, L. M. Beachan III, G. B. ELion, *J. Biol. Chem.* **1972**, *247*, 1597-1604.

[5] Nieminen, A. L.; Byrne, A. M.; Herman B.; Lemasters, J. *Am. J. Physiol. Cell Physiol.* **1997**, *272*, 1286-1294.

[6] B. Halliwell, J. M. C. Gutteridge, *Arch. Biochem. Biophys.* **1986**, *246*, 501-514.

Instruments: Fluorescence spectra were obtained by FluoroMax-4 Spectrofluorometer with a Xenon lamp and 1.0-cm quartz cells. Absorption spectra were measured on Lambda 35 UV-visible spectrophotometer (PerkinElmer). ^1H and ^{13}C NMR spectra were taken on a Bruker spectrometer. The fluorescence images of cells were taken using a LTE confocal laser scanning microscope (Germany Leica Co., Ltd) with objective lens (×20, ×40).

Absorption Analysis: Absorption spectra were obtained with 1.0-cm glass cells. The probe DA-Cy (acetonitrile, 0.05 mL, 1.0 mM) was added to a 10.0-mL color comparison tube. After dilution to 5 μM with 40 mM PBS buffers, then various concentrations H_2O_2 was added. The mixture was equilibrated for 7 min before measurement.

Fluorescence Analysis: Fluorescence emission spectra were obtained with a Xenon lamp and 1.0-cm quartz cells. The probe DA-Cy (acetonitrile, 0.05 mL, 1.0 mM) was added to a 10.0-mL color comparison tube. After dilution to 5 μM with 40 mM PBS buffers, H_2O_2 was added. The mixture was equilibrated for 7 min before measurement. The fluorescence intensity was measured simultaneously at $\lambda_{ex/em}$ = 630/755 nm, respectively. Another sample, the fluorescence recovery of DA-Cy, was oxidized by 50 μM H_2O_2, the mixture was equilibrated for 7 min, removed the redundant H_2O_2 by adding Vc, and then added various concentrations of GSH to equilibrate for 10 min at 37°C. The reaction was terminated by addition of 10 μL of pure trifluoroacetic acid.[6] Finally using 0.2 M PBS adjusted pH to 7.4 before measurement.

Confocal Imaging: Fluorescent images were acquired on a LSM510 confocal laser-scanning microscope (Germany Leica Co., Ltd) with an objective lens (×40). The excitation wavelength was 633 nm. Cell imaging was carried out after washing cells with fresh complete medium (RPMI-1640+20% FBS, 3×1 mL). HL-7702 cells were stained with 0.1 μM SYTO-16 green fluorescent nucleic acid dyes at 37 ^{o}C for 15min before obtaining live-cell molecular imaging.

Cell Culture: Human normal liver cell line (HL-7702 cells), human hepatoma cell line (HepG2 cells) and the mouse macrophage cell line (RAW264.7 cells) were maintained following protocols provided by the American Type Culture Collection. Cells were seeded at a density of 80% in visual field for confocal imaging in RPMI 1640 Medium supplemented with 20% fetal bovine serum (FBS), $NaHCO_3$ (2 g/L), and 1% antibiotics (penicillin /streptomycin, 100 U/ml). Cultures were maintained at 37 °C under a humidified atmosphere containing 5% CO_2. The cells were subcultured by scraping and seeding on 33 mm coverglass slides according to the instructions from the manufacturer.

Preparation and Staining of Fresh rat Hippocampal Slices. Slices were prepared from the hippocampi of 2-days-old rat (SD). Coronal slices were cut into 300 μm-thick using a vibrating-blade microtome in artificial cerebrospinal fluid (ACSF; 124 mM NaCl, 3 mM KCl, 26 mM $NaHCO_3$, 1.25 mM NaH_2PO_4, 10 mM D-glucose, 2.4 mM $CaCl_2$, and 1.3 mM $MgSO_4$). Slices were incubated with 5 μM DA-Cy in ACSF bubbled with 95% O_2 and 5% CO_2 for 6min at 37 °C.[7] Slices were then washed three times with ACSF and transferred to glass-bottomed dishes (MatTek) and observed in Olympus FV1000 confocal laser-scanning microscope with an objective lens (×10). The excitation wavelength was 635 nm. After incubated with 5 μM DA-Cy for 6min, the fresh rat hippocampal slices were washed with artificial cerebrospinal fluid (ACSF). Then the slices were incubated with 100 μM H_2O_2 for 9min to cause oxidative stress. Next, the slices were pre-incubated with α−lipoic acid (1 mM) for 3h, then washed and incubated with DA-Cy. To assess the effect of NEM, the slices were treated with 5 mM of NEM for 30 min before O-DA-Cy was added. Following this incubation, the slices were washed three times and imaged.

[7] Nita Patel, Yoshito Kumagai, Steven E. Unger, Jon M. Fukuto, Arthur K. Cho, *Chem. Res. Toxicol.*, **1991**, *4*, 421–426.

2. Synthesis and Characterization of Compounds

Synthesis of 2-{4-[2-(3,4-dihydroxyphenethyl)amino]-7-(1-ethyl-3,3-dimethyl(indolin-2-ylidene)}-3,5-(propane-1,3-diyl)-1,3,5-heptatrien-1-yl)-1-ethyl-3,3-dimethyl-3H-indolium(DA-Cy): Cy.7.Cl (1.00 g, 0.156 mmol), 4-(2-aminoethyl)benzene-1,2-diol hydrochloride (0.044 g, 0.234 mmol), and triethylamine (0.047 g, 0.468 mmol) were dissolved in 10 mL of anhydrous DMF in a 50-mL round bottom flask under Ar for 24 h at 90 ^{o}C.[8] Then the solvent was evaporated on a rotary evaporator until dry. The solid was purified on silica gel chromatography eluted with ethyl acetate/methanol (7:1 v/v). ^{1}H NMR (400 MHz, CD_3COCD_3-D_6) δ(ppm): 8.11 (s, 1H), 7.99 (m, 1H), 7.73-7.76 (m, 2H), 7.45-7.43 (m, 2H), 7.34-7.30 (m, 3H), 7.14-7.07 (m, 3H),6.86-6.53(m, 2H) 5.89-5.86 (d, 2H), 4.13-4.04 (m, 4H), 3.50-3.31 (m, 10H), 2.51-2.54 (m, 4H), 1.62-1.20 (m, 16H). ^{13}C NMR (CD_3COCD_3-D_6, 100 MHz) δ(ppm): 170.31,169.71, 163.71, 146.40, 144.94, 143.81, 141.28, 139.1, 131.65, 130.17, 129.32, 123.71, 123.15, 121.26, 121.13, 120.84, 117.04, 116.49, 116.22, 109.83, 95.18, 52.04, 48.59, 40.45, 37.97, 37.10, 35.88, 26.11, 21.14, 12.00. LC-MS (API-ES): *m*/*z* $C_{42}H_{50}N_3O_2^+$ Calcd 628.3898, found 628.3887.

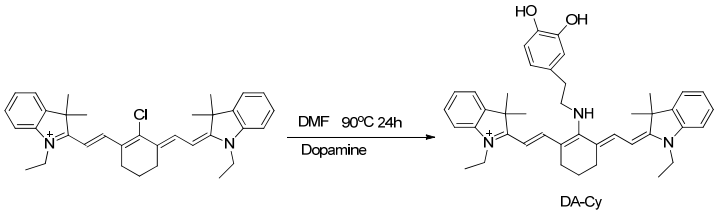

DA-Cy

Characterization of 2-{4-[2-((2-(3,4-dioxocyclohexa-1,5-dien-1-yl)ethyl)amino]-7-(1-ethyl- 3,3-dimethyl (indolin-2-ylidene)}-3,5-(propane-1,3-diyl)-1,3,5-heptatrien-1-yl)-1-ethyl-3,3-dimethyl-3H-indolium(O-DA-Cy): DA-Cy (0.01 g) was dissolved in 0.5 mL water. Subsequently, 10 equiv. of H_2O_2 was added. The mixture was equilibrated for 7 min, the redundant H_2O_2 was scavenged by adding ascorbic acid (100 mg) before tested. LC-MS (API-ES): *m*/*z* $C_{42}H_{48}N_3O_2^+$ Calcd 627.3825, found [M^+] 627.3818.

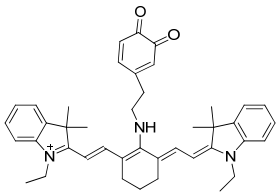

O-DA-Cy

Characterization of 2-{4-[2-(3,4-dihydroxy-5-(GSthio)phenethyl)amino]-7-(1-ethyl-3,3-dimethyl(indolin-2- ylidene)}-3,5-(propane-1,3-diyl)-1,3,5-heptatrien-1-yl)-1-ethyl-3,3-dimethyl-3H-indolium(GSH-DA-Cy): DA-Cy (0.01 mg) was dissolved in 0.5 mL water. Subsequently, 10 equiv. of H_2O_2 was added. The mixture was equilibrated for 7 min, the redundant H_2O_2 was scavenged by adding ascorbic acid (100 mg), adjusteded pH to 7.4 by 0.2 M PBS, and then added GSH (100 mg) to equilibrate for 10 min at 37°C.[9] The reaction was terminated by addition of pure trifluoroacetic acid (10 μL).[6] LC-MS (API-ES): *m*/*z* Calcd 933.4579, found [M^+] 933.5458.

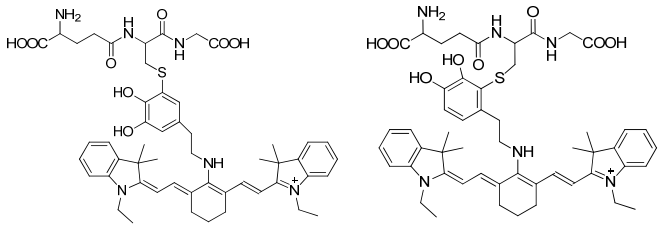

5-GSH-DA-Cy 99.3% 2-GSH-DA-Cy 0.7%

[8] Yu, F.; Li, P.; Li G.; Zhao, G.; Chu, T.; Han, K. J. Am. Chem. Soc. 2011, 133,11030.

[9] (a) Shen, X. M., Xia, B., Wrona, M. Z., Dryhurst, G. Chem. Res. Toxicol. 1996, 9, 1117-1126. (b) Zhang, F., Dryhurst, G. J. Med. Chem. 1994, 37, 1084-1098. (c) Spencer, J. P. E., Jenner, P., Daniel, S. E., Lees, A. J, Marsden, D. C., Halliwell, B. J. Neurochem. 1998, 71, 2112-2122. (d) Zhang, J., Kravtsov, V., Amarnath, V., Picklo, M. J., Graham, D. G., Montine, T. J. *J. Neurochem.* 2000, 74, 970-978.

HPLC Analyses of Oxidation Products and Addition Products. Cytoplasmic dopamine (DA) is normally autoxidized to DA-*o*-quinone as the resulting *o*-quinones are chemically reactive toward several cellular nucleophiles, with thiolates being greatly favored kinetically.[10] The products of thiolate addition to *o*-quinones are called catechol thioethers. In biological systems, catechol thioethers form mostly with free cysteine, GSH, or protein-bound cysteine at 5-position leading to formation of 5-*S*-thioldopamine.[11] Glutathione (GSH) is the most abundant endogenous thiol, whose concentration ranges from 1 to 15 mM depending on the cell types. However, the intracellular cysteine concentration is normally very low (~ 30 μM), since it is rapidly incorporated into GSH. Therefore, We anticipated that our probe mainly conjugated with GSH in cells. DA-Cy, O-DA-Cy, and GSH-DA-Cy were separated on a Skyway LC-310 HPLC system equipped with fluorescence and UV-vis absorption detectors. 20 μL of sample was injected into the HPLC system equipped with a C_{18} column (Alltech, Kromasil, 250 mm × 4.6 mm, 5 μm) equilibrated with CH_3CN. The compounds were separated with CH_3CN : water = 70 : 30 using a flow rate of 1 mL/min. Water phase contained 0.5% trifluoroacetic acid (TFA). Under those conditions O-DA-Cy eluted at 6.8 min, DA-Cy at 11.8 min, 5-GSH-DA-Cy (99.3%) at 21.8 min, 2-GSH-DA-Cy (0.7%) at 22.5

min. The peak areas detected by monitoring the absorption at 633 nm (DA-Cy, 5-GSH-DA-Cy, and 2-GSH-DA-Cy) and 520 nm (O-DA-Cy) were used in the quantitation.

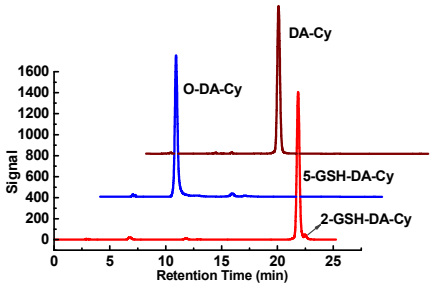

[10] (a) Zhang, J., Kravtsov, V., Amarnath, V., Picklo, M. J., Graham, D. G., Montine, T. J. *J. Neurochem.* 2000, 74, 970-978. (b) Tse D. C., McCreery R. L., and Adams R. N. *J. Med. Chem.* 1976, **19,** 37–40.

[11] (a) Montine T. J., Picklo M. J., Amarnath V., Whetsell W. O., Graham D. G. *Exp. Neurol.* 1997 **148,** 26–33. (b) Picklo M. J., Amarnath V., Graham D. G., Montine T. J. *Free Radic. Biol. Med.* 1999, *27***,** 271–277. (c) Lau, S. S., Hill, B. A., Highet, R. J., Monks, T. J. *Mo.l Pharmacol.* **1988**, *34*, 829-836. (d) Yu, J.; Wei, W.; Danner, E.; Ashley, R. K.; Israelachvili, J. N.; Waite, J. H. *Nat. Chem. Biol.* **2011**, *7*, 588.

3. Effect of pH Values

We evaluated the effect of pH on the fluorescence. The fluorescence of the probe was quenched along with pH increasing. However, as is shown in Fig. S1, the pH of the mediums hardly effects on fluorescence intensity within the range from 6.6 to 8.0. That is to say, the probe will work well under physiological conditions (pH=7.40, 40 mM PBS).

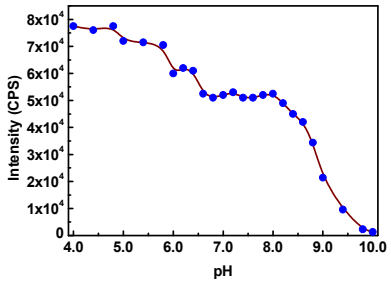

Fig. S1 The pH titration curve of the maximum fluorescence intensity changes DA-Cy (5 μM). pH 4.0, 4.4, 4.8, 5.0, 5.4, 5.8, 6.0, 6.2, 6.4, 6.8, 7.0, 7.2, 7.4, 7.6, 7.8, 8.0, 8.2, 8.4, 8.6, 8.8, 9.0, 9.4, 9.8, 10.0 (40 mM PBS buffer solution).

4. Coexist Various Biologically Relevant Analytes Interference Test

To study the specificity of DA-Cy toward H_2O_2, an important procedure was carried out to determine whether biologically relevant anion and cation other than H_2O_2 could potentially introduce signal noise. As shown in Fig. S2, no significant fluorescence intensity changes were observed in the emission spectra except in the case of H_2O_2. Now, we reported an on-off-on fluorescent probe for monitoring H_2O_2 oxidative stress and thiols reducing repair in living cells and tissues simply and directly, which could avoided a host of physiologically relevant ROS oxidants, anions, and cations.

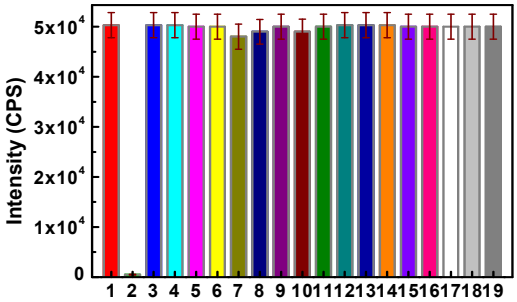

Fig. S2 The fluorescence intensity of DA-Cy (5 μM) at 755 nm excited at 630 nm in the presence of various biologically relevant analytes for 30 min. 1. Blank, 2. H_2O_2, 3. Na^+, 4. K^+, 5. Ca^{2+}, 6. Mg^{2+}, 7. Mn^{2+}, 8. Fe^{3+},9. Fe^{2+}, 10. Ni^{2+}, 11. Cu^{2+}, 12, Zn^{2+}, 13. Cl^-, 14, Br^-, 15. I^-, 16, SO_4^{2-}, 17, CO_3^{2-}, 18. NO_3^-, 19. Citrate. H_2O_2, Fe^{3+}, Fe^{2+}, and Cu^{2+} at 50 μM, all other analytes at 0.1 mM.

5. Kinetic Assays

Kinetic assays of the probe were performed within 1h. The results showed that the probe solution was stable to the medium, light, and air. Fig. S3 indicated that the probe could respond to the change of H_2O_2 within 7 min, and could conjugate with glutathione in 10 min by maintaining its fluorescent intensity. Taken together, DA-Cy was suitable for H_2O_2 oxidative stress and the GSH repair process monitoring. To check whether the chemoselective dopamine switch might turn off upon incubation with other ROS over time, the probe's time courses with various ROS for 30 min were measured. As Fig. S4 demonstrated, DA-Cy selectively responded to H_2O_2 by a turn-off fluorescence switch and avoided a host of other ROS oxidants.

It is a huge challenge to investigation the selective of fluorescence probes for reactive oxygen species.[12] Relative reactivities of one-electron oxidants are based on reduction potential and those of two-electron oxidants are based on reaction rates with antioxidants.[13] One-electron oxidants include H_2O_2, Hydroxyl radicals ($^{\cdot}OH$), Methyl linoleate hydroperoxide (MeLOOH), Cumene hydroperoxide (CuOOH), tert-Butylhydroperoxide (t-BuOOH), and $O_2^{\cdot-}$. Two-electron oxidants include $^1O_2$ and ClO^- in our test. Standard reduction potentials (E^o) are at pH 7. E^oDA/DA-o-quinone = ~ 0.9 V.[8] $E^oO_2^{\cdot-}/2H^+/H_2O_2$ = 0.94 V, $E^oROO^{\cdot}$, H^+/ROOH = 0.77 V, $E^oO_2/O_2^{\cdot-}$ =-0.16 V for 1 M oxygen, $E^oO_2^{\cdot-}/2H^+/H_2O_2 > E^o$DA/DA-o-quinone $> E^oROO^{\cdot}$, H^+/ROOH. These data show that H_2O_2 can oxidize DA more easily than other ROOH. Although $E^{o\cdot}OH$, H^+/H_2O = 2.31 V, its short lifetime might make it difficult to detect. $^1O_2$ and ClO^- are two-electron oxidants, E^oCl^-/OCl^- = 0.87 V,[9] E^oH_2O, H^+/O_2 = 1.22 V, however, they are based on reaction rates with DA. Above information may be the reason why our probe has specific for H_2O_2.

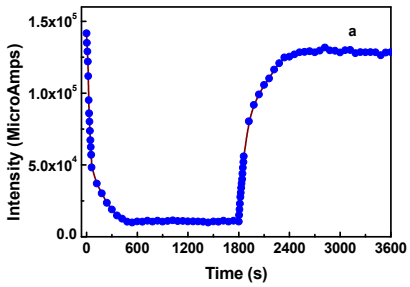

Fig. S3 Time course of DA-Cy (5 μM) as measured by a spectrofluorometer. DA-Cy was oxidized by 10 equiv of added H_2O_2 for 0.5h, after which the solution was treated with 1 mM of GSH for another half hour. All data were acquired in 40 mM PBS pH 7.4, λ_{ex} = 630 nm, λ_{em} = 755 nm.

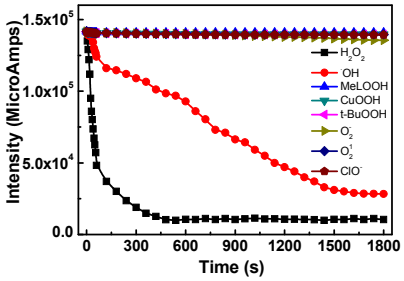

Fig. S4 Time courses of the responses of DA-Cy (5 μM) to diverse ROS for 30 min. 1, H_2O_2; 2, $^{\cdot}OH$ (; 3, methyl linoleate hydroperoxide (MeLOOH); 4, cumene hydroperoxide (CuOOH); 5, *tert*-butylhydroperoxide (t-BuOOH); 6, $O_2^{\cdot-}$; 7, $^1O_2$; 8, ClO^-. All ROS were at 50μM.

[12] a) X. Chen, X. Tian, I. Shin, J. Yoon, *Chem. Soc. Rev.* **2011**, *40*, 4783-4804. b) A. Gomes, E. Fernandes, J. L.F.C. Lima, *J. Biochem. Biophys. Methods* **2005**, 65,45–80. c) B. Halliwell, M. Whiteman, *Br. J. Pharmacol.* **2004**, 142, 231-255.

[13] C. C. Winterbourn, *Nat. Chem. Biol*. **2008**, 4, 278-286.

[14] Shen, X. M., Xia, B., Wrona, M. Z., Dryhurst, G. Chem. Res. Toxicol. 1996, 9, 1117-1126.

[15] a) G. R. Buettner, *Arch. Biochem. Biophys.* **1993**, 300, 535–543. b) M. D. Bartberger, W. Liu, E. Ford, K. M. Miranda, C. Switzer, J. M. Fukuto, P. J. Farmer, D. A. Wink, K. N. Houk, *Proc. Natl. Acad. Sci. USA* **2002**, 99, 10958–10963.

6. Limit of H_2O_2 and GSH Detection

Limit of detection in analysis.[16] The limit of detection, expressed as the concentration c_L, or the quantity q_L, is derived from the smallest measure x_L, that can be detected with reasonable certainty for a given analytical procedure. The value of x_L is given by the equation:

$$x_L = \bar{x}_{bi} + k s_{bi} \quad (1)$$

Where $\bar{x}_{bi}$ is the mean of the blank measures, s_{bi} is the standard deviation of the blank measures, and k is a numerical factor chosen according to the confidence level desired.

$$c_L = \frac{(x_L - \bar{x}_B)}{m} \quad (2)$$

Where, m is the slope of the linear regression equation.
Combine two of the equations, Long and Winefordner defined c_L:

$$c_L = \frac{(k \cdot s_B)}{m} \quad (3)$$

Generally, κ=3, $P < 0.01$, we obtained c_L = 0.3 μM for H_2O_2 and GSH for 1.0 μM.

[16] IUPAC. Compendium of Chemical Terminology, 2nd ed. (the "Gold Book"). Compiled by A. D. McNaught and A. Wilkinson. Blackwell Scientific Publications, Oxford (1997). XML on-line corrected version: http://goldbook.iupac.org (2006) created by M. Nic, J. Jirat, B. Kosata; updates compiled by A. Jenkins. ISBN 0-9678550-9-8.

7. Absorption and Emission Spectra for GSH Reduction Processes

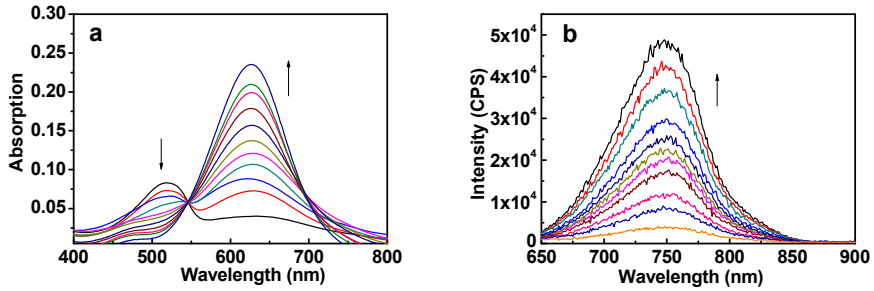

Fig. S5 Absorption spectra and fluorescence responses of 5 μM O-DA-Cy to various concentrations of added GSH: 0, 0.05, 0.1, 0.15, 0.2, 0.25, 0.3, 0.35, 0.4, 0.45, 0.5 mM. Spectra were acquired in 40 mM PBS, pH 7.4 at 25°C after incubation of the probe with GSH for 10 min (λ_{ex} = 630 nm, λ_{em} = 755 nm). a) O-DA-Cy displayed one major absorption band centered at 520 nm. Upon addition of H_2O_2, a new absorption peak appeared at 630 nm with isosbestic point at 535 nm. b) Corresponding NIR fluorescence emission spectra respond to various [GSH].

8. Absorption and Fluorescence Response of Cy.7.Cl to H_2O_2

Among the near-infrared fluorescent dyes, cyanine fluorochromes have got more and more attention. Quite a number of functional cyanine probes have been developed.[17] However, the central polymethine chain of cyanine dyes could be oxidatively cleaved.[18] It hypothesized that H_2O_2 might also react with cyanine dye and reduce its fluorescence. Therefore, we evaluated the Cy.7.Cl's fluorescence response towards 50 μM H_2O_2 for 1h. As Fig. S3 indicates the fluorescent intensity undergoes unobvious optical changes in terms of absorption spectra variation and fluorescence intensity. The results provide satisfactory information that the probe can do a good job under the given conditions and can tolerate superfluous H_2O_2 in certain extent.

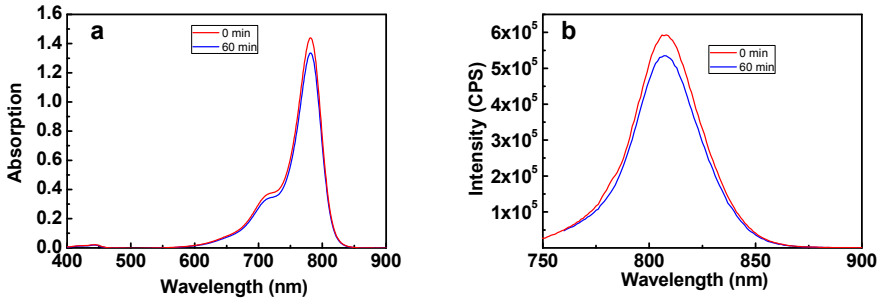

Fig. S6 Absorption spectra and fluorescence responses of 5 μM Cy.7.Cl to 50 μM H_2O_2 for 1h. Spectra were acquired in 40 mM PBS, pH 7.4 at 25°C (λ_{ex} = 790 nm, λ_{em} = 815 nm).

[17] K. Kiyose, H. Kojima, T. Nagano, *Chem.-Asian J.* **2008**, *3*, 506–515.

[18] D. Oushiki, H. Kojima, T. Terai, M. Arita, K. Hanaoka, Y. Urano, T. Nagano, *J. Am. Chem. Soc.*, **2010**, *132*, 2795–2801.

9. MTT Assay

3-(4,5-Dimethylthiazol-2-yl)-2,5-diphenyltetrazolium bromide (MTT) assay: HL-7702 cells (10^6 cell mL^{-1}) were dispersed within replicate 96-well microtiter plates to a total volume of 200 μL $well^{-1}$. Plates were maintained at 37 °C in a 5% CO_2/95% air incubator for 4h. HL-7702 cells were then incubated for 24h upon different concentrations probe of 10^{-3}, 10^{-4}, 10^{-5}, 10^{-6}, 10^{-7} and 10^{-8} M respectively. MTT solution (5.0 mg/mL, PBS) was then added to each well. After 4h, the remaining MTT solution was removed, and 200 μL of DMSO was added to each well to dissolve the formazan crystals. Absorbance was measured at 570 nm in a TRITURUS microplate reader. Calculation of IC50 values was done according to Huber and Koella.[19]

[19] W. Huber, J. C. Koella, *Acta Trop.* **1993**, *55*, 257–261.

10. The Time-Dependence of the Probe Location in Cells

The optimization of incubating with probe was performed. The point at 3 min was selected out. These data establish that DA-Cy is good membrane-permeable.

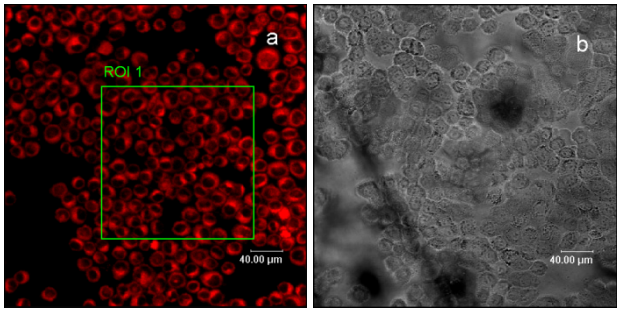

Fig. S7 Confocal fluorescence images of HL-7702 cells with times: cells incubated with DA-Cy (5 μM), the total time is 10 min; (b) Bright field image. ROI1: the green region.

Table S1. Fluorescence intensity at various times

Time / Data / Region	30 s	60 s	90 s	120 s	180s	240 s	300 s	360 s
ROI 1	5.02	9.05	17.06	24.83	36.69	36.56	36.58	36.67

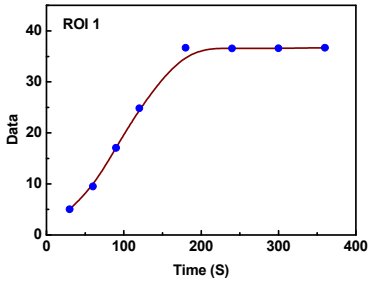

Fig. S8 Nonlinear fitting of the time-dependence of the location of the probe in HL-7702 cells.

11. Bright-Field, and SYTO-16 dye Images of Fig. 4

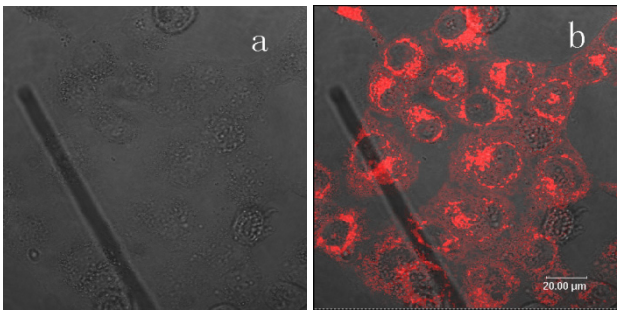

Fig. S9 Live-cell molecular imaging shows that DA-Cy localized to cytoplasm in live HL-7702 cells. (a) Brightfield of Fig. 4a. (b) Merged images of brightfield (a) and red (Fig. 4a) channel.

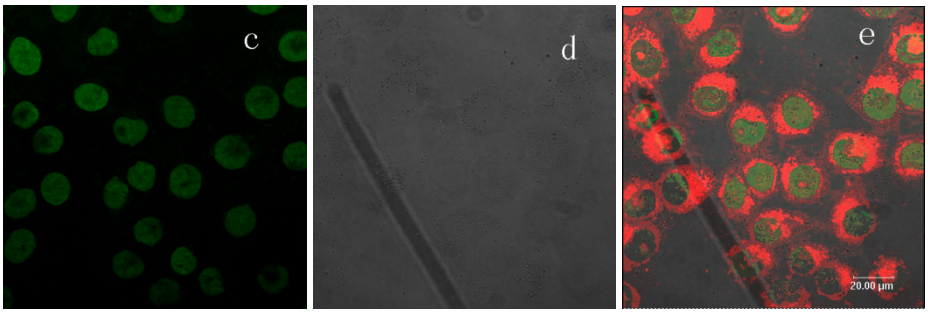

Fig. S10 Live-cell molecular imaging shows that DA-Cy colocalized to cytoplasm in live HL-7702 cells. (c) Co-staining with SYTO-16 dye images and (d) Bright-field of Fig. 4c. (e) Merged bright-field (d), 0.1 µM SYTO-16 dye (c) green, and Fig. 4c red channels.

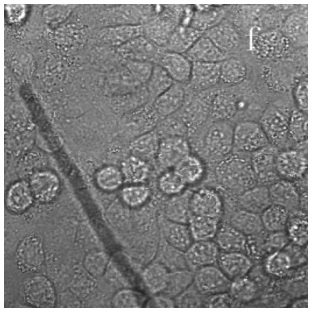

Fig. S11 (f) Brightfield of Fig. 4b.

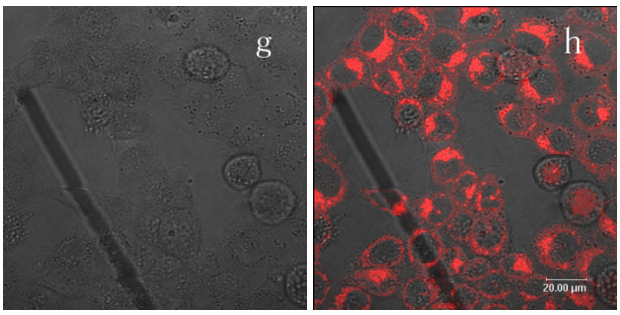

Fig. S12 Live-cell molecular imaging shows that DA-Cy localized to cytoplasm in live HL-7702 cells. (g) Brightfield of Fig. 4d. (h) Merged images of brightfield (g) and Fig. 4d red channel.

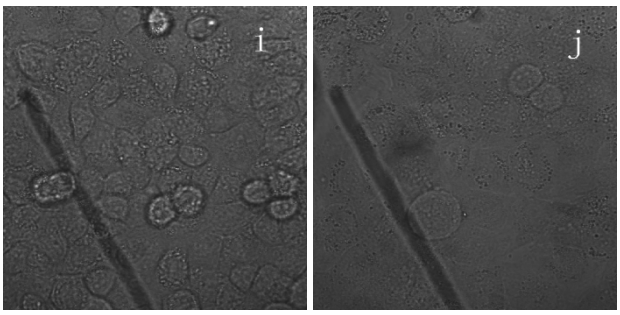

Fig. S13 (i) Brightfield of Fig. 4e. (j) Brightfield of Fig. 4f.

12. Characterize Thiols Reducing Repair Capability in Different Types of Cell Line

After establishing that DA-Cy could sense the H_2O_2 oxidation and monitor thiols reducing repair in HL-7702 cells, we used this new chemical tool to characterize thiols reducing repair capability in different types of cell lines. It was well-known that normal hepatocytes kept high levels of GSH and protein thiols, while the concentration declined severely in injured ones caused by oxidative stress. We applied DA-Cy to both HL-7702 and HepG2 cells.

After incubated with the probe (5 μM) for 3 min, both cells lines showed strong intracellular fluorescence (Fig. S12g, S12j). After addtion of 25 μM H_2O_2 for 9 min, the two cells lines were washed with fresh complete medium for 3 times. Two types of cell lines showed negligible intracellular fluorescence because of the burst of H_2O_2 oxidative stress (Fig. S12h, S12k). Cells were washed with fresh complete medium once again, then maintained in the incubator at 37°C and 5% CO_2 atmosphere for 3h, and HL-7702 cells showed a clear increase in the intracellular fluorescence intensity (Fig. S12i), while HepG2 cells only showed weaker fluorescence (Fig. S12l). The results demonstrated that the HL-7702 cells and HepG2 cells conserved different cellular thiols pools and had different thiols repair capabilities. Our probe was able to sense the different intracellular redox environments in the different types of cells.

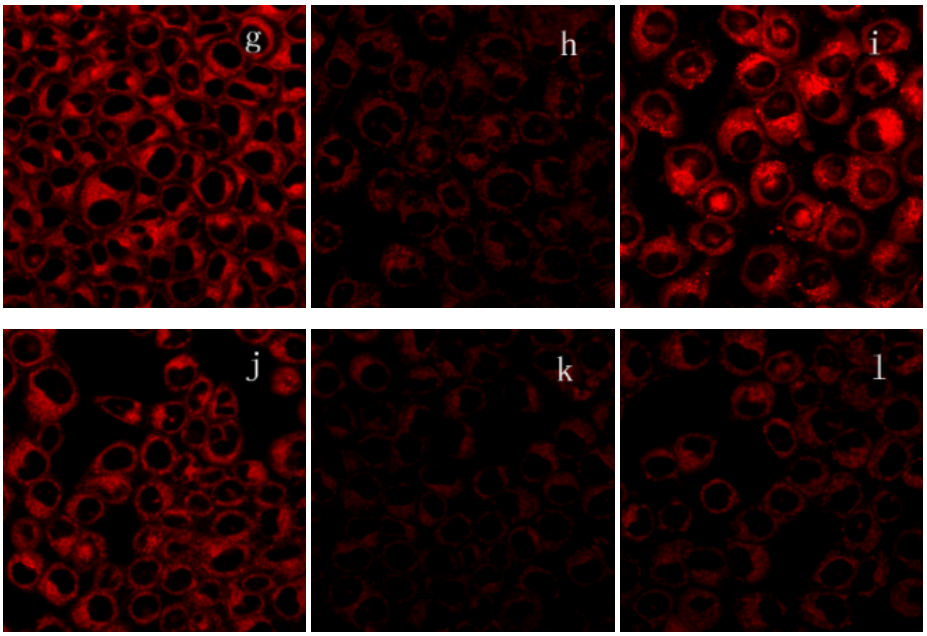

Fig. S14 Application of DA-Cy to demonstrate different thiols repair capacities in HL-7702 and HepG2 cells. (g) HL-7702 cells incubated with 5 μM DA-Cy for 3 min. (h) Dye-loaded cells treated with 25 μM H_2O_2 for 9 min. (i) Cells as described in (h) after an additional 3h. (j) HepG2 cells loaded with DA-Cy (5 μM) for 3 min. (k) Probe-loaded cells treated with 25 μM H_2O_2 for 9 min. (l) Treated cells as described in (k) after a further culture for 3h.

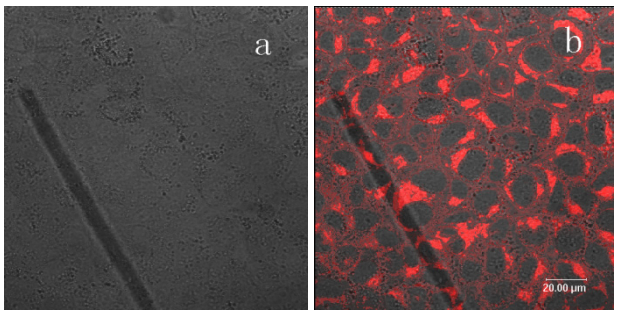

Fig. S15 Live-cell molecular imaging shows that DA-Cy localized to cytoplasm in live HL-7702 cells. (a) Brightfield of Fig. S14g. (b) Merged images of brightfield (a) and Fig. S14g red channel.

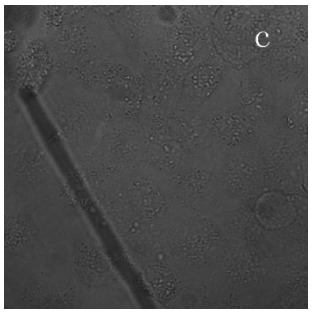

Fig. S16 (c) Brightfield of Fig. S14h.

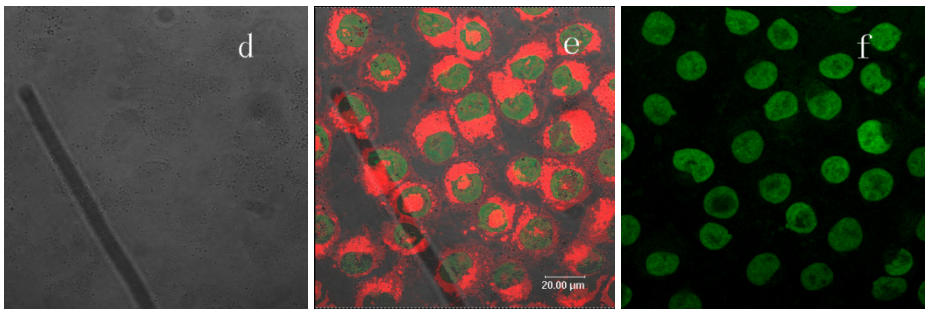

Fig. S17 Live-cell molecular imaging shows that DA-Cy colocalized to cytoplasm in live HL-7702 cells. (d) Brightfield, and Stained by 0.1 μM SYTO-16 dye (f) Images of Fig. S14i. (e) Overlay bright-field (d), SYTO-16 dye (f) green and red Fig. S14i channels.

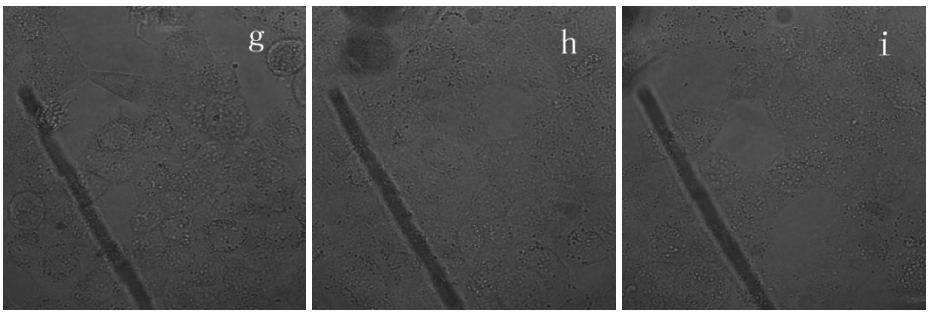

Fig S18 (g) Brightfield of Fig. S14j. (h) Brightfield of Fig. S14k. (i) Brightfield of Fig. S14l.

13. Comparisons with Other Hydrogen Peroxide Probes

In order to further established DA-Cy was a good membrane-permeable and could respond to H_2O_2 oxidation/thiols reducing repair process by modulating fluorescent switch on-off-on in living cells. We Cooperated DA-Cy with other two hydrogen peroxide probes, one is PF6-AM by Chang, the other is DCFH derivatives by Maeda. The experimental study includes 3 parallel control groups. RAW264.7 cells in Fig. S20 and S23 were incubated with DA-Cy, PF6-AM, and DCFH derivatives (all in 5 μM) for 30 min. The cells showed strong intracellular fluorescence in red channel (Fig. S20a and S23a) and faint intracellular fluorescence in green channel (Fig. S20b and S23b) because of the reducing cytosolic environment. RAW264.7 cells in Fig. S19 and S20 were incubated with phorbol 12-myristate 13-acetate (PMA, 1 μg/mL) for 30 min at 37 °C, then loaded DA-Cy, PF6-AM, and DCFH derivatives (all in 5 μM) for another 30 min. Prompt decreases in red channel (Fig. S20a and S24a) and rapid increase in channel green (Fig. S21b and S24b) were observed as the probes sensed the burst of H_2O_2 oxidative stress. RAW264.7 cells in Fig. S22 and S24 were first treated as in Fig. S21 and S24 then incubated with glutathione S-transferase (GST, 125 U/mL) and α-lipoic acid for 15 min. The fast recovery of fluorescence intensity showed DA-Cy detected thiols reducing repair process in cells. The blue fluorescent Hoechst dyes are cell permeable nucleic acid stains (Fig. S20c, S21c, S22a, S23c, S24c, and S25a). The fluorescence of these dyes is very sensitive to DNA conformation and chromatin state in cells. The results indicated our probe is a good candidate for H_2O_2 oxidation-thiols reduction process in cells.

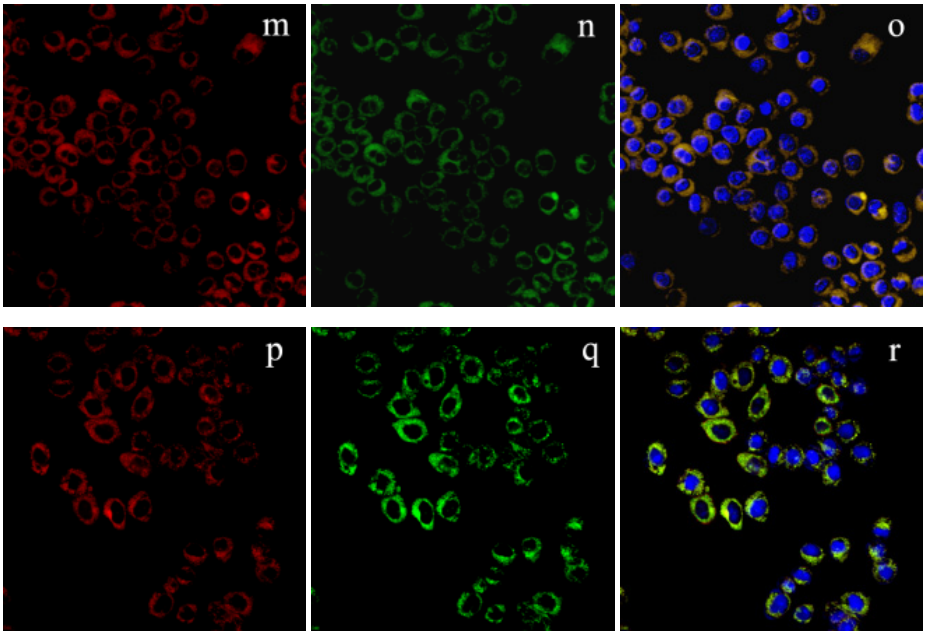

Fig. S19 Comparisons with the analytical performance of other H_2O_2 probes in RAW264.7 cells. (m) and (p) DA-Cy (5 μM) loaded cells treated with phorbol 12-myristate 13-acetate (PMA, 1 μg/mL) for 30 min at 37 °C, incubated with glutathione S-transferase (GST, 125 U/mL) and α-lipoic acid for 15 min. (n) and (q) Costained with H_2O_2 probe PF6-AM and DCFH derivatives (all 5 μM), respectively. (o) and (r) Merged red, green and blue channels. Blue channel collected by stained with Hoechst dye.

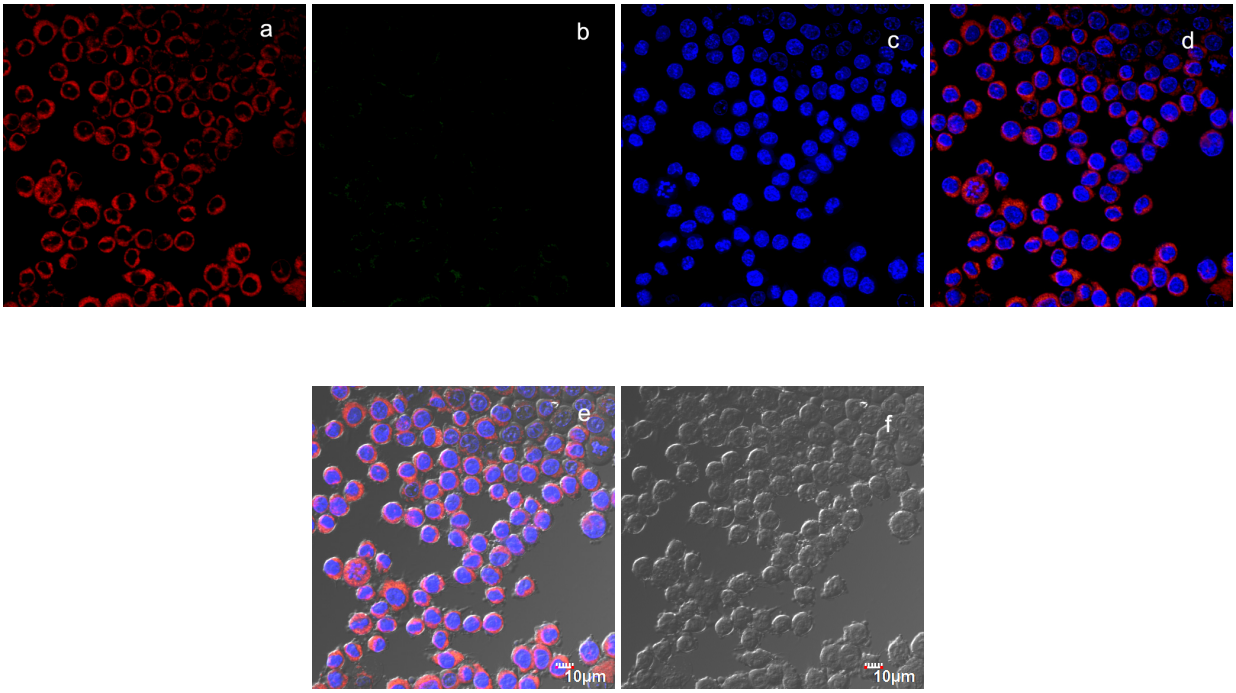

Fig. S20 RAW264.7 cells loaded with 5 μM DA-Cy and 5 μM PF6-AM. (a) Red channel with DA-Cy. (b) Green channel with PF6-AM. (c) Blue channel with hoechst dye. (d) Merged red, green and blue channels. (e) Merged red, green, blue channels and brightfield. (f) brightfield of (a).

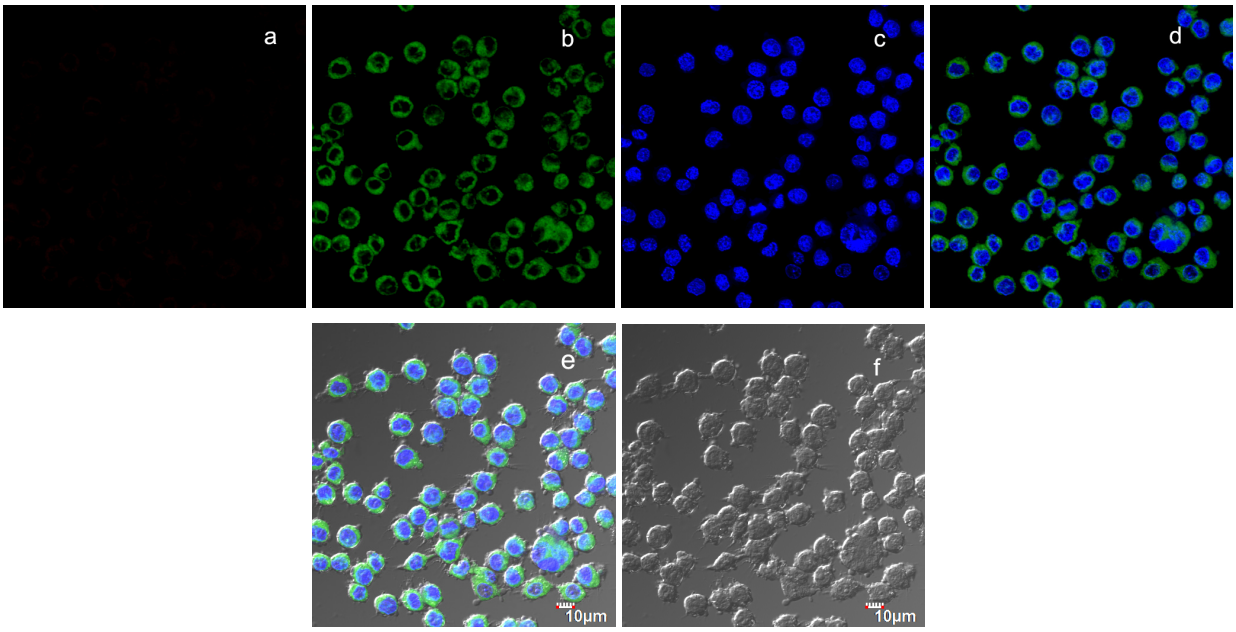

Fig. S21 RAW264.7 cells loaded with 5 μM DA-Cy and 5 μM PF6-AM, the treated with phorbol 12-myristate 13-acetate (PMA, 1 μg/mL) for 30 min at 37 °C. (a) Red channel with DA-Cy. (b) Green channel with PF6-AM. (c) Blue channel with hoechst dye. (d) Merged red, green and blue channels. (e) Merged red, green, blue channels and brightfield. (f) brightfield of (a).

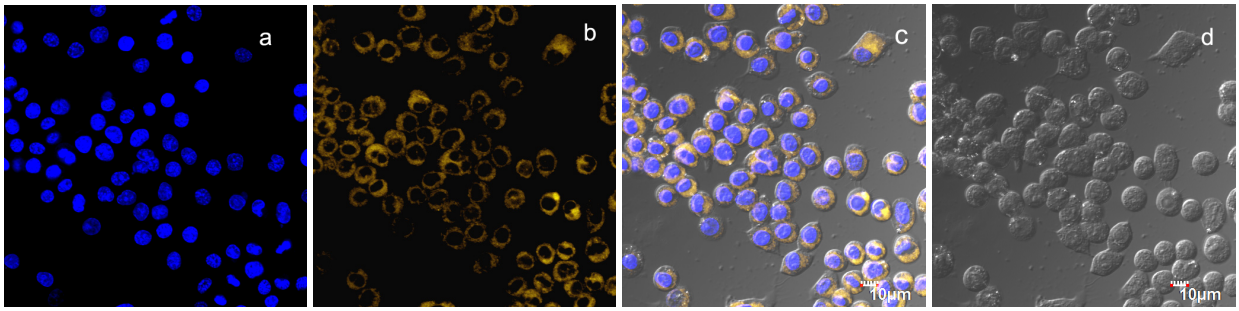

Fig. S22 More images of Fig. 6. (a) Blue channel with hoechst dye. (b) Merged red (6m) and green (6n) channels. (c) Merged red (6m) and green (6n) and brightfield. (d) brightfield of (Fig. 6m).

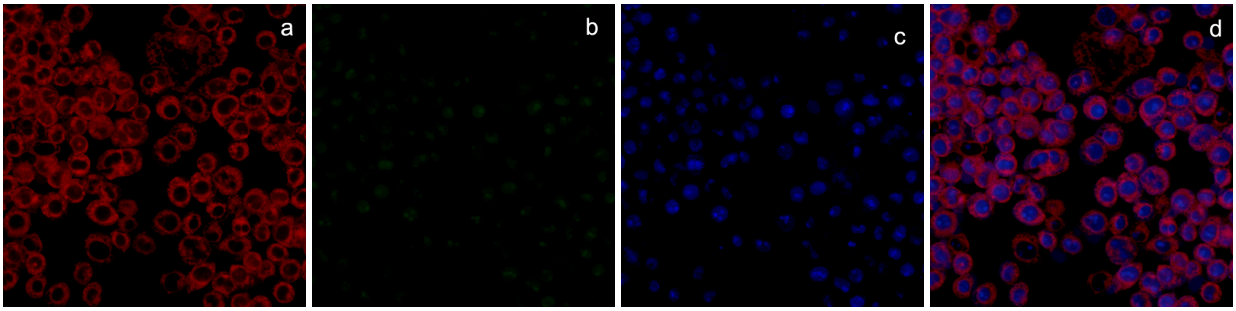

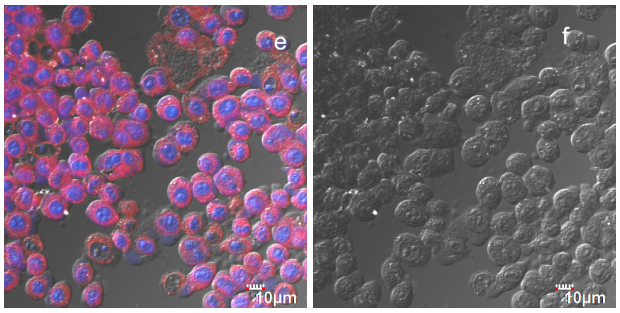

Fig. S23 RAW264.7 cells loaded with 5 μM DA-Cy and 5 μM DCFH derivatives. (a) Red channel with DA-Cy. (b) Green channel with DCFH derivative. (c) Blue channel with hoechst dye. (d) Merged red, green and blue channels. (e) Merged red, green, blue channels and brightfield. (f) brightfield of (a).

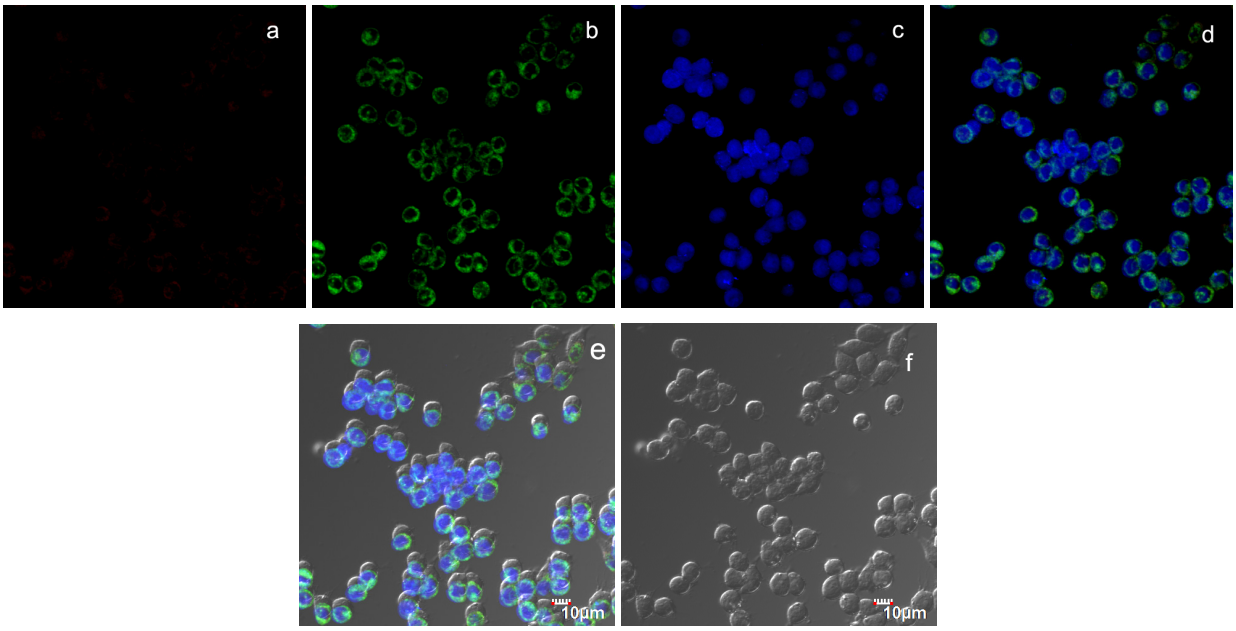

Fig. S24 RAW264.7 cells loaded with 5 μM DA-Cy and 5 μM DCFH derivatives, the treated with phorbol 12-myristate 13-acetate (PMA, 1 μg/mL) for 30 min at 37 °C. (a) Red channel with DA-Cy. (b) Green channel with DCFH derivatives. (c) Blue channel with hoechst dye. (d) Merged red, green and blue channels. (e) Merged red, green, blue channels and brightfield. (f) brightfield of (a).

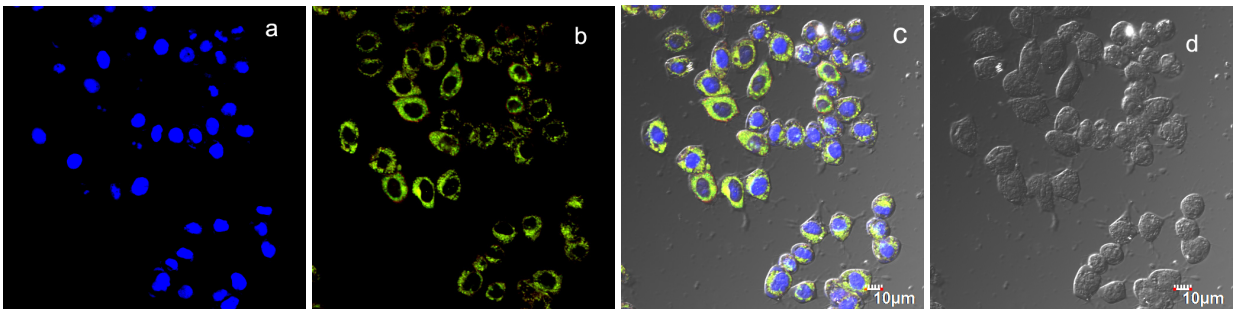

Fig. S25 More images of Fig. 6. (a) Blue channel with hoechst dye. (b) Merged red (6p) and green (6q) channels. (c) Merged red (6p) and green (6q) and brightfield. (d) brightfield of (Fig. 6p).

14. Bright-Field Images of Fresh Rat Hippocampal Slices

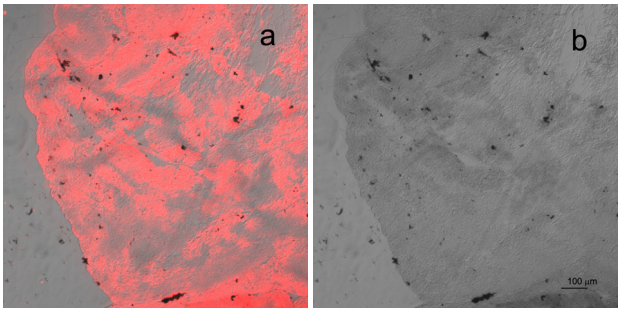

Fig.S26 (a) Overlay bright-field (b) and red Fig. 7s channels. (b) Brightfield of Fig. 5g.

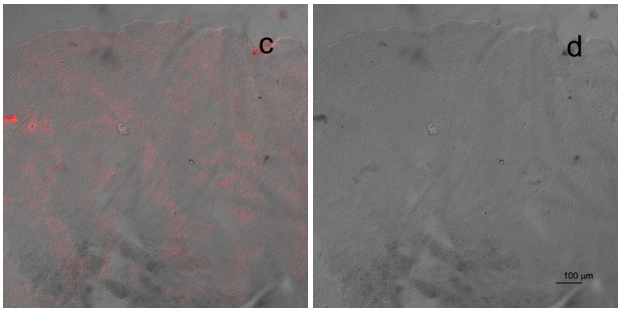

Fig. S27 (c) Overlay bright-field (d) and red Fig. 7t channels. (d) Brightfield of Fig. 5h.

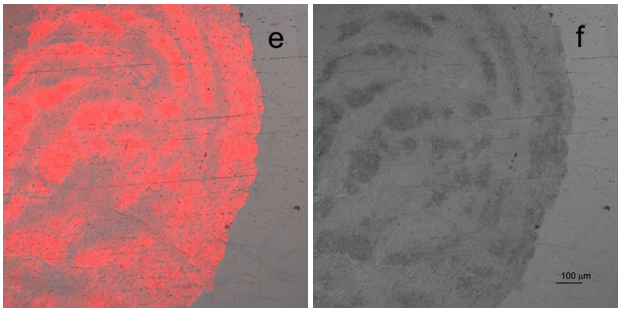

Fig.S28 (e) Overlay bright-field (f) and red Fig. 7u channels. (f) Brightfield of Fig. 5i.

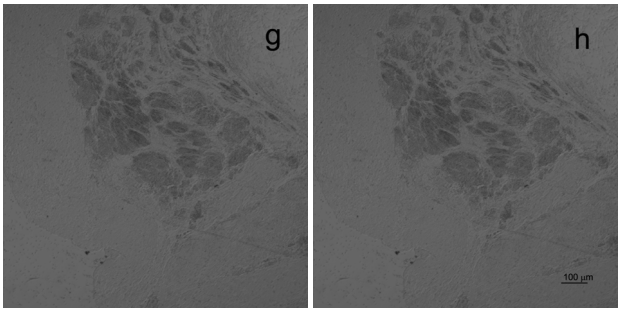

Fig. S29 (g) Overlay bright-field (h) and red Fig. 7v channels. (h) Brightfield of Fig. 5j.

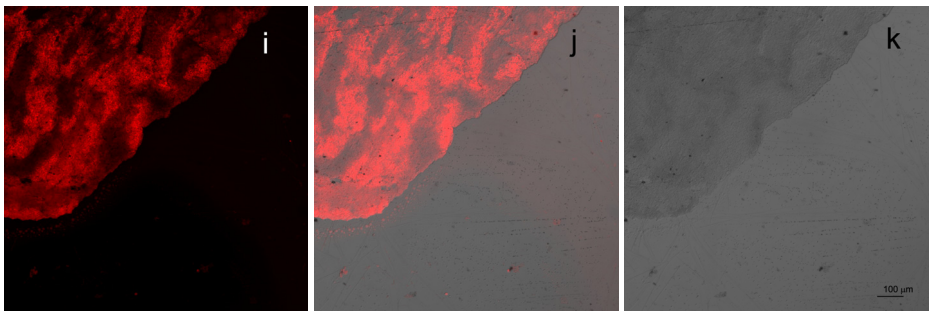

Fig. S30 (i) Hippocampal slice treated with 100 μM H_2O_2 for 9 min, incubated with α-lipoic acid, and then stained by 5 μM O-DA-Cy. (j) Overlay bright-field (k) and red Fig. S30i channels. (k) Brightfield of Fig. S30i.

15. Theoretical and Computational Methods

Our data suggested that the detection mechanism relied on photoinduced electron transfer process from the excited fluorophore to the *o*-quinone moiety (donor-excited PET, d-PET).[20] The mechanism was proved to be effective via the density functional theory calculations of DA-Cy, O-DA-Cy, and GSH-DA-Cy (BP86 functional with TZVP basis sets using Gaussian 09 package).[21] Here, excitation energies and oscillator strengths (*f*) were defined to evaluate electronic excited states and photophysical properties of the probe. For molecular DA-Cy, the calculating results displayed that low-lying transition-allowed S_0–S_1 excitation was the transition from the highest occupied molecular orbital (HOMO) to the lowest unoccupied molecular orbital (LUMO), both of which resided on Cy moiety (f = 1.9189), and the S_1 state of DA-Cy could release strong fluorescence while back to the S_0 state (Fig. S29a). The calculations of GSH-DA-Cy gave very similar results with those of DA-Cy (Fig. S29c). The S_0–S_1 transaction was f =1.8181. Upon oxidized by H_2O_2, the *d*-PET process occurred from cyanine moiety to DA-*o*-quinone unit in the S_1 state of molecular O-DA-Cy. A small oscillator strength of S_0–S_1 excitation (f = 0.0013) inferred a forbidden transition. In other words, the S_1 state of O-DA-Cy could not be directly excited from its S_0 state (Fig. S29b). However, it might be populated by internal conversion from its S_3 state, due to the maximum oscillator strength f = 1.9587 of the S_0–S_3 excitation. These calculations were consistent with the experimental results and rationalized the *d*-PET process.

[20] A. P. de Silva, H. Q. Gunaratne, T. Gunnlaugsson, A. J. Huxley, C. P. McCoy, J. T. Rademacher, T. E. Rice, *Chem. Rev.* **1997**, 97, 1515. (b) T. Ueno, Y. Urano, K. Setsukinai, H. Takakusa, H. Kojima, K. Kikuchi, K. Ohkubo, S. Fukuzumi, T. Nagano, *J. Am. Chem. Soc.* **2004**, 126, 14079.

[21] The Gaussian 09 package refer to Gaussian 09, Revision A.02, M. J. Frisch, G. W. Trucks, H. B. Schlegel, G. E. Scuseria, M. A. Robb, J. R. Cheeseman, G. Scalmani, V. Barone, B. Mennucci, G. A. Petersson, H. Nakatsuji, M. Caricato, X. Li, H. P. Hratchian, A. F. Izmaylov, J. Bloino, G. Zheng, J. L. Sonnenberg, M. Hada, M. Ehara, K. Toyota, R. Fukuda, J. Hasegawa, M. Ishida, T. Nakajima, Y. Honda, O. Kitao, H. Nakai, T. Vreven, J. A. Montgomery, Jr., J. E. Peralta, F. Ogliaro, M. Bearpark, J. J. Heyd, E. Brothers, K. N. Kudin, V. N. Staroverov, R. Kobayashi, J. Nor-mand, K. Raghavachari, A. Rendell, J. C. Burant, S. S. Iyengar, J. Tomasi, M. Cossi, N. Rega, J. M. Millam, M. Klene, J. E. Knox, J. B. Cross, V. Bakken, C. Adamo, J. Jaramillo, R. Gomperts, R. E. Stratmann, O. Yazyev, A. J. Austin, R. Cammi, C. Pomelli, J. W. Ochterski, R. L. Martin, K. Morokuma, V. G. Zakrzewski, G. A. Voth, P. Salvador, J. J. Dannenberg, S. Dapprich, A. D. Daniels, O. Farkas, J. B. Foresman, J. V. Ortiz, J. Cioslowski, and D. J. Fox, Gaussian, Inc., Wallingford CT, **2009**.

Theoretical details: For the theoretical study of photophysics of DA-Cy, O-DA-Cy and GSH-DA-Cy, we used the Gaussian 09 program package**.** The ground state geometries of DA-Cy, O-DA-Cy and GSH-DA-Cy were optimized by the density functional theory (DFT) employing the Becke's three-parameter hybrid exchange functional with Lee-Yang-Parr gradient-corrected correlation (B3LYP functional),[22] and the triple-ζ valence quality with one set of polarization functions (TZVP)[23] as basis sets. The excited state geometry of DA-Cy, O-DA-Cy and GSH-DA-Cy were optimized employing the time-dependent density functional theory (TD-DFT). No constrains for symmetry, bonds, angles, or dihedral angles were applied in the geometry optimization calculations. All the local minima were confirmed by the absence of an imaginary mode in vibrational analysis calculations.

[22] (a) A. D. Becke, J. Chem. Phys. 1993, 98, 5648. (b) P. A. M. Dirac, Proc. Royal Soc. (London) A 1929, 123, 714. (c) S. H. Vosko, L. Wilk, M. Nusair, Can. J. Phys. 1980, 58, 1200. (d) A. D. Becke, Phys. Rev. A 1988, 38, 3098. (e) C. Lee, W. Yang, R. G. Parr, Phys. Rev. B 1988, 37, 785.

[23] O. Treutler, R.Ahlrichs, J. Chem. Phys. 1995, 102, 346.

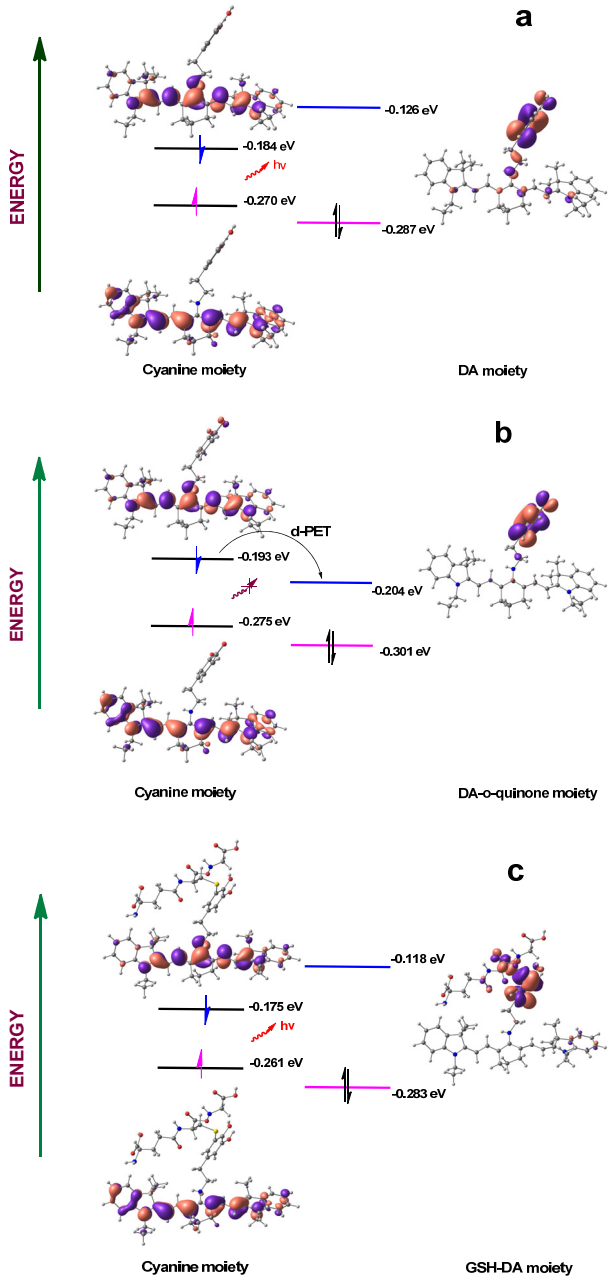

Fig. S31 Frontier molecular orbital energy illustrations show the relative energetic dispositions of the orbitals of two moieties in DA-Cy, O-DA-Cy and GSH-DA-Cy.

Calculated Electronic Transitions Energies

Table S2. Calculated electronic transitions energies for **DA-Cy**, **O-DA-Cy** and **5-GSH-DA-Cy** obtained from TD-DFT/B3LYP/TZVP calculations

Transitions	λ_{cal} (nm)	λ_{exp} (nm)	f	CI expansion coefficients
DA-Cy				
S_0–S_1	550		1.9189	0.709 (HOMO → LUMO)
S_0–S_2	508		0.0167	0.699 (HOMO-1 → LUMO)
S_0–S_3	441		0.0237	0.681 (HOMO-2 → LUMO)
S_0–S_4	382		0.0022	0.705 (HOMO-3 → LUMO)
S_0–S_5	336		0.0448	0.544 (HOMO-4 → LUMO)
				0.386 (HOMO-5 → LUMO)
S_0–S_6	336		0.0377	0.556(HOMO-5 → LUMO)
				-0.359(HOMO-4 → LUMO)

O-DA-Cy			
S_0–S_1	764	0.0003	0.701 (HOMO → LUMO)
S_0–S_2	693	0.0002	0.689 (HOMO-2 → LUMO)
S_0–S_3	658	1.9587	0.704 (HOMO→ LUMO+1)
			0.286 (HOMO-1 → LUMO)
S_0–S_4	529	0.0248	0.698 (HOMO-1 → LUMO)
S_0–S_5	444	0.0214	0.686 (HOMO-1 → LUMO+1)
S_0–S_6	397	0.0009	0.549 (HOMO-2 → LUMO+1)
			0.413 (HOMO-8 → LUMO)
GSH-DA-Cy			
S_0–S_1	550	1.8181	0.709 (HOMO → LUMO)
S_0–S_2	476	0.0225	0.638 (HOMO-1 → LUMO)
			-0.302 (HOMO-2 → LUMO)
S_0–S_3	439	0.0375	0.626 (HOMO-2→ LUMO)
			0.286 (HOMO-1 → LUMO)
S_0–S_4	396	0.0001	0.706 (HOMO-3 → LUMO)
S_0–S_5	341	0.0267	0.610 (HOMO-5 → LUMO)
			-0.318 (HOMO-7 → LUMO)
S_0–S_6	340	0.0122	0.695 (HOMO-4 → LUMO+1)

XYZ Coordinates (angstrom) and SCF Energies (a.u.)

Note: upper case letters before the atomic coordinates indicate the atomic symbol of the atoms involved in the calculations.

DA-Cy

Energy = -1945.7360847

C	-0.498872	3.188648	0.211601
C	0.739447	2.521728	0.474272
C	0.736945	1.117572	1.051378
C	-0.659575	0.517223	1.213081
C	-1.549821	0.929350	0.037252
C	-1.709917	2.431071	0.054075
C	1.936606	3.100361	0.079580
C	3.210974	2.538989	0.260679
C	4.405644	3.023675	-0.246649
C	4.655352	4.282360	-1.099722
C	6.159319	4.220615	-1.295619
C	6.662939	3.096462	-0.648210
N	5.596488	2.394985	-0.046951
C	-2.946100	3.047015	-0.010553
C	-4.182020	2.432989	-0.291177
C	-5.420555	3.046180	-0.303887
C	-5.784484	4.505852	0.033704
C	-7.293932	4.487752	-0.133841
C	-7.698382	3.215519	-0.528222
N	-6.565788	2.384101	-0.638868
C	-6.658558	0.978714	-1.031404
C	-6.836327	0.028369	0.152165
C	5.797832	1.158873	0.708838
C	6.036625	1.394567	2.199797
N	-0.524056	4.543427	0.025448
C	0.207910	5.560817	0.786163
C	-0.747556	6.524489	1.511377
C	-0.002331	7.613925	2.246199
C	0.448513	8.744344	1.558242

C	1.165094	9.736792	2.209269
C	1.441500	9.604790	3.577447
C	0.999644	8.489297	4.269218
C	0.280784	7.496182	3.605277
C	-9.031298	2.904611	-0.760696
C	-9.968484	3.923550	-0.590194
C	-9.579118	5.201539	-0.199989
C	-8.231660	5.490565	0.030597
C	8.016207	2.787309	-0.649547
C	8.870809	3.648863	-1.337110
C	8.381680	4.774393	-1.994117
C	7.015835	5.067130	-1.975385
C	-5.159370	5.497291	-0.972499
C	-5.412058	4.870017	1.486230
C	4.276165	5.573590	-0.343053
C	3.933557	4.198326	-2.462536
O	2.152727	10.642825	4.128594
O	1.585489	10.828233	1.516065
H	1.322672	0.473659	0.386081
H	1.258576	1.108996	2.014508
H	-0.586157	-0.570126	1.281018
H	-1.121319	0.864446	2.141448
H	-1.098638	0.591809	-0.903174
H	-2.517240	0.436996	0.117473
H	1.867937	4.034052	-0.458380
H	3.267739	1.635786	0.851523
H	-2.973428	4.109990	0.188667
H	-4.162247	1.381121	-0.537371
H	-7.499619	0.893547	-1.719315
H	-5.767322	0.727039	-1.605912
H	-6.908603	-0.999594	-0.207288
H	-7.746513	0.257561	0.707697
H	-5.993263	0.089663	0.841562
H	4.932545	0.516549	0.547366
H	6.648420	0.645508	0.261086
H	6.192026	0.439424	2.704347
H	5.183683	1.890689	2.664509
H	6.920647	2.012035	2.363333
H	-1.338897	4.897433	-0.450460
H	0.846482	5.058001	1.509335
H	0.857165	6.136758	0.120848
H	-1.425937	6.973667	0.777993
H	-1.361732	5.953940	2.212310
H	0.234533	8.881889	0.504658
H	1.209428	8.394390	5.329246
H	-0.066887	6.633455	4.160840
H	-9.349284	1.914688	-1.058451
H	-11.015777	3.711455	-0.763361
H	-10.324588	5.975651	-0.073280
H	-7.937258	6.488126	0.334281
H	8.410926	1.919566	-0.138798
H	9.931842	3.435398	-1.356294
H	9.064485	5.427864	-2.521198
H	6.643027	5.945890	-2.487936
H	-5.532177	6.503097	-0.773733
H	-5.424217	5.235170	-1.997244
H	-4.072542	5.522903	-0.898144

H	-5.794107	5.864109	1.722902
H	-4.333295	4.877632	1.640698
H	-5.851463	4.163357	2.190985
H	4.580778	6.441847	-0.929003
H	4.779960	5.625538	0.622660
H	3.203543	5.644183	-0.171443
H	4.227183	5.046150	-3.083350
H	2.850095	4.221444	-2.349913
H	4.202067	3.283754	-2.992536
H	2.250898	10.528370	5.080100
H	2.037550	11.428145	2.125814

O-DA-Cy

Energy = -1944.4746497

C	-0.459162	3.219608	0.179726
C	0.775309	2.560975	0.461455
C	0.772523	1.185341	1.101828
C	-0.626932	0.612344	1.323081
C	-1.537838	0.970417	0.145288
C	-1.676147	2.473173	0.073206
C	1.972722	3.119397	0.030495
C	3.245903	2.571226	0.238822
C	4.440079	3.026206	-0.302514
C	4.682318	4.228544	-1.234427
C	6.185441	4.158298	-1.432620
C	6.694312	3.078181	-0.718371
N	5.630726	2.414603	-0.068179
C	-2.907480	3.100276	-0.036008
C	-4.145364	2.482616	-0.284451
C	-5.381685	3.103983	-0.336262
C	-5.736138	4.580692	-0.072862
C	-7.244900	4.564525	-0.243897
C	-7.656757	3.276865	-0.574297
N	-6.527831	2.433548	-0.638663
C	-6.630006	1.009142	-0.957469
C	-6.823708	0.125254	0.273825
C	5.840415	1.232892	0.769933
C	6.089602	1.572947	2.238670
N	-0.458139	4.572891	-0.086469
C	0.197589	5.601492	0.720644
C	-0.808223	6.398478	1.580552
C	-0.119524	7.452132	2.408277
C	-0.109842	8.749418	2.042045
C	0.607459	9.769260	2.820396
C	1.355007	9.286615	4.103851
C	1.264517	7.849885	4.419148
C	0.582380	7.013310	3.621795
C	-8.990552	2.961921	-0.795010
C	-9.921487	3.993967	-0.679083
C	-9.524764	5.287753	-0.352816
C	-8.176503	5.580483	-0.133180
C	8.047617	2.770352	-0.706291
C	8.897543	3.588234	-1.450244
C	8.403460	4.670233	-2.173754
C	7.037475	4.962130	-2.167842
C	-5.101117	5.518311	-1.123456
C	-5.365002	5.009741	1.362145

C	4.302649	5.564431	-0.559052
C	3.954227	4.056275	-2.585438
O	1.971555	10.071654	4.786106
O	0.639143	10.935829	2.498660
H	1.336269	0.504902	0.454128
H	1.315868	1.213982	2.052562
H	-0.565195	-0.470445	1.448599
H	-1.065043	1.014652	2.240778
H	-1.114301	0.570673	-0.783470
H	-2.510306	0.499554	0.277154
H	1.895424	4.021451	-0.559201
H	3.305512	1.703368	0.880263
H	-2.922187	4.174223	0.093188
H	-4.134142	1.417695	-0.466565
H	-7.467445	0.895521	-1.645525
H	-5.737402	0.720845	-1.511988
H	-6.905919	-0.919181	-0.031687
H	-7.733833	0.393008	0.811887
H	-5.983106	0.213004	0.963386
H	4.975834	0.579194	0.659588
H	6.688848	0.691844	0.351990
H	6.250197	0.655587	2.807432
H	5.238965	2.099094	2.673705
H	6.973698	2.201219	2.352603
H	-1.260752	4.906523	-0.597136
H	0.934183	5.118576	1.357949
H	0.734462	6.297222	0.070432
H	-1.544535	6.873000	0.927612
H	-1.342365	5.700982	2.232523
H	-0.628491	9.101342	1.157337
H	1.767560	7.513329	5.317293
H	0.523591	5.959956	3.876429
H	-9.313935	1.960224	-1.043257
H	-10.969644	3.780177	-0.844328
H	-10.265851	6.071648	-0.267624
H	-7.876980	6.590377	0.120412
H	8.445909	1.936648	-0.144254
H	9.958792	3.375606	-1.461052
H	9.083083	5.290500	-2.743287
H	6.661627	5.806686	-2.732907
H	-5.471040	6.534019	-0.976678
H	-5.361635	5.207556	-2.135581
H	-4.014407	5.543195	-1.044940
H	-5.737418	6.017727	1.550441
H	-4.286520	5.012108	1.519252
H	-5.813710	4.342032	2.098238
H	4.606126	6.394339	-1.198630
H	4.807929	5.677436	0.400714
H	3.229376	5.644395	-0.392862
H	4.243300	4.863362	-3.260106
H	2.871340	4.084077	-2.468816
H	4.222945	3.110491	-3.057188

GSH-DA-Cy

Energy = -3425.269502

C	-4.804972	2.887927	3.724530
C	-3.635357	2.069352	3.580598

C	-3.724644	0.577144	3.855734
C	-5.140308	0.074081	4.140236
C	-6.150675	0.833079	3.274827
C	-6.109206	2.288575	3.675478
C	-2.460780	2.591997	3.066236
C	-1.277218	1.863601	2.843120
C	-0.133553	2.315500	2.209906
C	0.170540	3.712283	1.634165
C	1.576257	3.517626	1.094150
C	1.991031	2.213433	1.347968
N	0.952000	1.517189	1.998193
C	-7.245411	2.979602	4.059864
C	-8.575640	2.559211	3.873689
C	-9.717054	3.165747	4.367110
C	-9.844572	4.335756	5.361041
C	-11.351805	4.433550	5.520919
C	-11.962989	3.463144	4.732779
N	-10.969647	2.733059	4.047385
C	-11.291007	1.632016	3.141865
C	-11.370041	0.275445	3.841856
C	1.074392	0.115857	2.396099
C	1.607747	-0.066054	3.816675
N	-4.715136	4.244384	3.828055
C	-3.655839	5.055074	4.429515
C	-4.239693	6.193703	5.279604
C	-3.158658	7.110440	5.806284
C	-2.526941	8.020664	4.950715
C	-1.519666	8.850199	5.414041
C	-1.128091	8.786275	6.759599
C	-1.750790	7.882078	7.617700
C	-2.755531	7.038117	7.135052
C	-13.342094	3.313099	4.681381
C	-14.110332	4.188056	5.449692
C	-13.512207	5.169293	6.235396
C	-12.121044	5.299445	6.277462
C	3.247485	1.754029	0.977348
C	4.093054	2.650536	0.323928
C	3.690390	3.955956	0.057537
C	2.422754	4.397599	0.445114
C	-9.291248	5.661133	4.795158
C	-9.182477	3.982666	6.710961
C	0.181461	4.788738	2.741360
C	-0.796420	4.090473	0.491820
O	-0.151775	9.659980	7.139352
O	-0.927713	9.735043	4.566171
H	-3.337613	0.047353	2.978759
H	-3.061071	0.311377	4.685546
H	-5.192795	-0.999818	3.948396
H	-5.398770	0.224045	5.191810
H	-5.903200	0.700919	2.215164
H	-7.146895	0.421252	3.423525
H	-2.472662	3.626318	2.761096
H	-1.261469	0.842172	3.194777
H	-7.098026	3.927231	4.562480
H	-8.724602	1.676802	3.267716
H	-12.243190	1.873363	2.669251
H	-10.547442	1.619305	2.345394

H	-11.623364	-0.500784	3.117579
H	-12.136281	0.278427	4.617901
H	-10.418573	0.011801	4.305578
H	0.098996	-0.356648	2.281052
H	1.734596	-0.365657	1.675038
H	1.678492	-1.129549	4.051574
H	0.949944	0.401980	4.549983
H	2.601431	0.371057	3.922672
H	-5.561589	4.750622	3.620837
H	-3.026548	4.411014	5.043322
H	-3.019166	5.494407	3.656329
H	-4.940056	6.770944	4.665041
H	-4.808314	5.775895	6.112591
H	-2.821674	8.112425	3.911752
H	-3.247375	6.356622	7.816486
H	-13.818601	2.552691	4.077479
H	-15.189123	4.098506	5.430655
H	-14.130272	5.839013	6.819467
H	-11.664543	6.064290	6.894519
H	3.576896	0.744532	1.182647
H	5.079024	2.321084	0.021940
H	4.363859	4.633231	-0.451209
H	2.117043	5.415975	0.236761
H	-9.541643	6.474136	5.477561
H	-9.729280	5.888090	3.822406
H	-8.206865	5.639700	4.689048
H	-9.435280	4.730681	7.463263
H	-8.096723	3.930181	6.619774
H	-9.538001	3.017321	7.074775
H	0.504789	5.742585	2.322061
H	0.872997	4.520619	3.540882
H	-0.804742	4.931065	3.179990
H	-0.466572	5.021604	0.028804
H	-1.814645	4.236234	0.850967
H	-0.813508	3.318441	-0.278212
H	-0.014574	9.562099	8.097391
H	-0.277335	10.251153	5.063028
N	-4.741439	7.721434	11.386205
H	-5.027724	8.092244	12.281615
C	-3.324184	7.479848	11.199853
H	-3.185530	6.473466	10.799937
C	-2.708455	8.488165	10.199368
C	-2.667248	7.558230	12.574246
H	-3.440910	8.684753	9.422942
H	-2.455509	9.426537	10.692447
S	-1.200325	7.833842	9.331393
O	-3.225952	7.923307	13.580733
O	-1.381491	7.193233	12.514535
N	-10.300898	5.657495	9.955559
H	-11.285420	5.844737	9.808014
C	-9.563793	6.874208	10.281274
H	-9.764166	7.253680	11.295034
C	-8.052330	6.577877	10.150556
C	-10.019000	7.971937	9.330585
H	-7.889714	5.593725	10.597144
H	-7.796211	6.471456	9.096523
C	-7.108954	7.582560	10.808842

O	-10.790392	7.829507	8.414805
H	-7.310606	8.593028	10.445243
H	-7.256184	7.607806	11.892380
C	-5.654387	7.273608	10.481804
O	-5.312748	6.699474	9.454790
O	-9.470103	9.170213	9.632956
H	-9.817794	9.818323	8.999036
H	-10.211488	4.976496	10.699780
N	-0.718167	7.131589	13.806825
H	-1.248143	7.753039	14.420863
C	0.628842	7.648531	13.597203
C	1.202931	8.033698	14.945329
H	1.255149	6.893809	13.123443
H	0.649348	8.548426	12.967525
O	0.543667	8.320833	15.909596
O	2.548014	8.054569	14.915902
H	2.861266	8.354277	15.784966